Advanced Synthesis & Catalysis

Accepted Article

Title: An Enzymatic 2-Step Cofactor and Co-Product Recycling Cascade towards a Chiral 1,2-Diol. Part II: Catalytically Active Inclusion Bodies

Authors: Vera D. Jäger, Maja Piqueray, Selina Seide, Martina Pohl, Wolfgang Wiechert, Karl-Erich Jaeger, and Ulrich Krauss

To be cited as: *Adv. Synth. Catal.* 10.1002/adsc.201900189

Link to VoR: http://dx.doi.org/10.1002/adsc.201900189

10.1002/adsc.201900189

FULL PAPER

DOI: 10.1002/adsc.201((will be filled in by the editorial staff))

An Enzymatic 2-Step Cofactor and Co-Product Recycling Cascade towards a Chiral 1,2-Diol. Part II: Catalytically Active Inclusion Bodies

Vera D. Jäger[a,c], Maja Piqueray[a], Selina Seide[b,c], Martina Pohl[b,c], Wolfgang Wiechert[b,c], Karl-Erich Jaeger[a,b,c], Ulrich Krauss[a,c*]

[a] Institut für Molekulare Enzymtechnologie, Heinrich-Heine-Universität Düsseldorf, Forschungszentrum Jülich, 52425 Jülich, Germany [Corresponding author: Ulrich Krauss: Phone: +49-2461-61-2939; Fax: +49-2461-61-2490, Email: u.krauss@fz-juelich.de]
[b] Forschungszentrum Jülich GmbH, IBG-1: Biotechnology, 52425 Jülich, Germany
[c] Bioeconomy Science Center (BioSC), c/o, Forschungszentrum Jülich, 52425 Jülich, Germany

Received: ((will be filled in by the editorial staff))

Supporting information for this article is available on the WWW under http://dx.doi.org/10.1002/adsc.201######.

Abstract

Optimal performance of multi-step enzymatic one-pot cascades requires a facile balance between enzymatic activity and stability of multiple enzymes under the employed reaction conditions. We here describe the optimization of an exemplary two-step one-pot recycling cascade utilizing the thiamine diphosphate (ThDP)-dependent benzaldehyde lyase from *Pseudomonas fluorescens* (*Pf*BAL) and the alcohol dehydrogenase from *Ralstonia* sp. (*R*ADH) for the production of the vicinal 1,2-diol (1*R*,2*R*)-1-phenylpropane-1,2-diol (PPD) using both enzymes as catalytically active inclusion bodies (CatIBs). *Pf*BAL is hereby used to convert benzaldehyde and acetaldehyde to (*R*)-2-hydroxy-1-phenylpropanone (HPP), which is subsequently converted to PPD. For recycling of the nicotinamide cofactor of the *R*ADH, benzyl alcohol is employed as cosubstrate, which is oxidized by *R*ADH to benzaldehyde, establishing a recycling cascade. In particular the application of the *R*ADH, required for both the reduction of HPP and the oxidation of benzyl alcohol in the recycling cascade is challenging, since the enzyme shows deviating pH optima for reduction (pH 6-10) and oxidation (pH 10.5), while both enzymes show only low stability at pH >8. This inherent stability problem hampers the application of soluble enzymes and was here successfully addressed by employing CatIBs of *Pf*BAL and *R*ADH, either as single, independently mixed CatIBs, or as co-immobilizates (Co-CatIBs). Single CatIBs, as well as the Co-CatIBs showed improved stability compared to the soluble, purified enzymes. After optimization of the reaction pH, the *R*ADH/*Pf*BAL ratio and the co-solvent content, we could demonstrate that almost full conversion (>90%) was possible with CatIBs, while under the same conditions the soluble enzymes yielded at most >50% conversion. Our study thus provides convincing evidence that (Co-)CatIB-immobilizates can be used efficiently for the realization of cascade reactions, i.e. under conditions where enzyme stability is a limiting issue.

Keywords: inclusion bodies, enzyme immobilization, protein co-localization, biocatalysis, synthetic reaction cascades

Introduction

Optically pure 1,2-diols represent valuable building blocks for the production of pharmaceuticals, chemical catalysts, and agrochemicals.[1] Apart from using chemical methods,[2] they can be obtained biocatalytically from either prochiral α-hydroxy ketones, by NAD(P)H-dependent alcohol dehydrogenases (ADHs),[3] or by combining the carboligation of aldehydes by thiamine diphosphate (ThDP)-dependent enzymes with ADHs in a cascade reaction.[4] For example, by combining a set of different ThDP-dependent enzymes with different ADHs all four stereoisomers of 1-phenyl-1,2-propanediol have been obtained,[4a] and the production of the vicinal 1,2-diol (1*R*,2*R*)-1-phenylpropane-1,2-diol (PPD), a precursor of the calcium channel blocker diltiazem [5] was optimized, by employing either purified, isolated enzymes in aqueous media [6] or by using whole cells in microaqueous organic solvent.[4a, 4b] Here, a two-step one-pot reaction cascade for the synthesis of (PPD, **4**) was realized using the benzaldehyde lyase of *Pseudomonas fluorescens* (*Pf*BAL) and the alcohol dehydrogenase from *Ralstonia* sp. (*R*ADH) starting from benzaldehyde **1** and acetaldehyde **2** yielding (*R*)-2-hydroxy-1-phenylpropanone (HPP, **3**) as an intermediate. The use of benzyl alcohol **5** as a co-substrate for the substrate-coupled regeneration of the nicotinamide cofactor (NADPH) results in recycling of benzaldehyde **1**, which can then by reused in the carboligation reaction of the first step (Scheme 1, A). The general functionality of such a recycling cascade has been shown in part I of this paper by employing

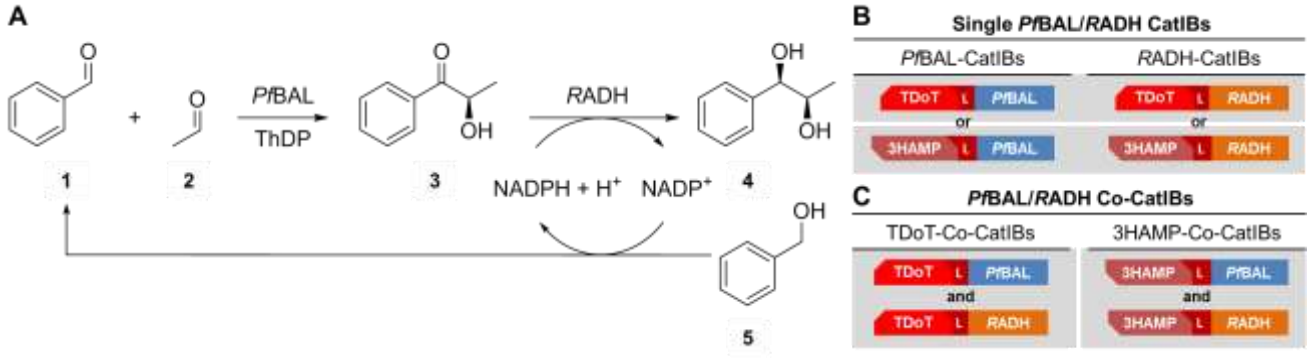

Scheme 1. Two-enzyme one-pot cascade for the synthesis of (1*R*,2*R*)-1-phenylpropane-1,2-diol (A). In the first step, *Pf*BAL catalyzes the carboligation of benzaldehyde **1** and acetaldehyde **2** to yield the intermediate (*R*)-2-hydroxy-1-phenylpropanone (HPP, **3**). In the second step, HPP is reduced by *R*ADH to yield (1*R*,2*R*)-1-phenylpropane-1,2-diol (PPD, **4**). *R*ADH requires NADPH as a cofactor, which is regenerated in a co-substrate driven approach utilizing the oxidation of benzyl alcohol **5** to yield the benzaldehyde substrate **1** for the *Pf*BAL reaction. Schematic illustration of the fusion constructs used in this study for the generation single *Pf*BAL/*R*ADH CatIBs (B) and the corresponding Co-CatIBs (C). (Co-)CatIB formation is achieved by molecular biological fusion of two different coiled-coil domains (TDoT and 3HAMP; dark and light red) to *Pf*BAL (blue) and *R*ADH (orange) via a linker polypeptide (L; dark red) constituted by 3-fold GlyGlyGlySer repeat and a Factor Xa protease cleavage site. For the generation of Co-CatIBs both gene fusions were co-expressed in *E. coli*, which results in the co-immobilization of the two enzymes within inclusion body (IB) particles. CatIBs that were used together in cascade reactions are marked by grey boxes.

soluble, purified *Pf*BAL and *R*ADH.[6] However, only suboptimal conversions were observed, which we speculate is most probably due to stability issues of the two soluble enzymes in the cascade. Several stability studies of *Pf*BAL have been performed in the past, indicating that specifically the contact with the aldehyde substrates like benzaldehyde and acetaldehyde causes fast inactivation in batch processes.[7] Further, using *R*ADH for both the reduction of HPP and the oxidation of benzyl alcohol in the recycling cascade is challenging, since the enzyme shows deviating pH optima for reduction (pH 6-10) and oxidation (pH 10.5), but only low stability at pH >8.[8]

To address those stability issues, we have recently developed a simple and efficient strategy to immobilize enzymes in catalytically active inclusion bodies (CatIBs) directly in the *E. coli* production cell. Thereby, CatIB formation is induced by aggregation-inducing tags such as the tetrameric coiled-coil domain of the cell surface protein Tetrabrachion (tetramerization domain of tetrabrachion; TDoT) from the from *Staphylothermus marinus* [9] or the dimeric 3HAMP coiled-coil domain (belonging to the family of signaling domains found in histidine kinases, adenylyl cyclases, methyl-accepting chemotaxis proteins, and phosphatases), derived from the soluble oxygen sensor Aer2 from *Pseudomonas aeruginosa*.[10] Both have previously been employed to induce CatIB formation for a variety of enzymes and fluorescent proteins,[11] among those also *Pf*BAL and *R*ADH.[11a, 11b] As demonstrated earlier, fusion of TDoT and 3HAMP to these enzymes, resulting in the fusion proteins TDoT-L-*Pf*BAL, 3HAMP-L-*Pf*BAL, TDoT-L-*R*ADH, and 3HAMP-L-*R*ADH (L denoting the presence of an interdomain linker polypeptide consisting of a 3-fold GlyGlyGlySer repeat and a Factor Xa protease cleavage site)(Scheme 1, B), yielded in all cases the formation of CatIBs.[11c] We also demonstrated recently that both enzymes can be jointly produced in TDoT-based Co-CatIBs (Scheme 1, C, left), although the activity specifically of the *R*ADH in these Co-CatIBs was not yet optimal.[11b] As we could demonstrate that 3HAMP-based CatIBs are generally much more active compared to TDoT-based CatIBs,[11a, 11c] we here evaluate 3HAMP-based Co-CatIBs as well as the single CatIBs of both enzymes as an alternative to the cascade with soluble enzymes for the synthesis of the chiral 1,2-diol PPD **4** (Scheme 1, A). The stability of all enzyme preparations was additionally studied relative to the soluble enzymes under reaction conditions to delineate potential stabilizing effects caused by immobilization in (Co-)CatIBs. We demonstrate that due to the higher stability of *Pf*BAL and *R*ADH in CatIBs the conversion of the cascade in batch could be optimized to reach >90 % conversion, while accumulating only marginal amounts of the HPP by-product, which can be attributed to the higher stability of the CatIBs making reactions at 30 °C possible (compared to 20 °C chosen in part I of this paper [6]).

Results and Discussion

Modulation of the (Co-)CatIB properties by different coiled-coil domains

As a first step to improve cascade performance, we compared a set of different single CatIBs of *Pf*BAL and *R*ADH (Scheme 1, B) as well as different Co-CatIBs (Scheme 1, C), the latter containing both enzymes in a fixed ratio.

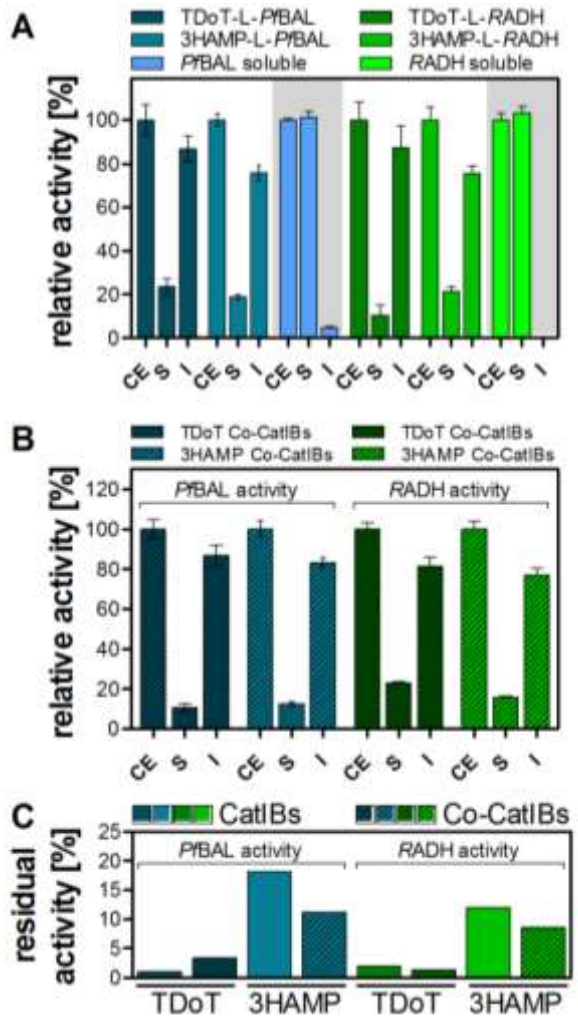

Figure 1. Distribution of *Pf*BAL and *R*ADH activity in cellular fractions after cell lysis of *E. coli* BL21(DE3) producing (A) single *Pf*PBAL- and *R*ADH-CatIBs as well as (B) the corresponding Co-CatIBs. CE: crude cell extract, S: soluble protein-containing fraction, I: insoluble inclusion bodies (IBs) containing fraction. The SDS-PAGE analysis illustrating the 3HAMP Co-CatIBs purification procedure is shown in ESI Figure S5. (C) Residual activity of the TDoT- and 3HAMP-(Co-)CatIBs. Residual activity was determined based on k_{cat}; relative to the activity of the corresponding soluble purified enzyme (see ESI, Table S1). For details see Experimental Section. Error bars correspond to the standard deviation of the mean derived from at least three technical relicates of three independent biological triplicates. Except the data for the 3HAMP Co-CatIBs, the depicted data has been presented previously.[11a-c]

As previously shown for TDoT Co-CatIBs ([11b]; data also shown for comparison in Figure 1, B), co-expression of the 3HAMP-L-*Pf*BAL and 3HAMP-L-*R*ADH encoding gene fusions resulted in the formation of Co-CatIBs, as can be deduced from the high respective enzymatic activities in the insoluble IB-containing cellular fraction (I) (Figure 1B; for SDS-PAGE analysis see ESI, Figure S5).The observed CatIB-formation efficiency, defined as the activity of the respective enzyme in the insoluble inclusion body (IB)-containing fraction relative to the activity of the crude cell extract (set to 100%), was very similar for all analyzed fusion enzymes (in all cases >70% of the activity was found in the insoluble IB-containing fraction), but huge differences were observed with regard to the specific activities of the (Co-)CatIBs. Whereas all TDoT-derived (Co-)CatIBs showed low residual activities (1.0% and 3.3%) compared to the corresponding purified soluble enzymes, the 3HAMP-derived (Co-)CatIBs retained much higher residual activities (8.6% and 18.1%) (Figure 1, C and ESI Table S1). Overall, the residual activity of both *Pf*BAL and *R*ADH appears to be lower in the 3HAMP Co-CatIBs relative to the corresponding single 3HAMP CatIBs (Figure 1, C and Table S1). In conclusion, the higher activity observed for the 3HAMP (Co-)CatIBs compared to the TDoT (Co-)CatIBs highlights the possibility to tailor the properties of CatIBs by fusion of different coiled-coil domains. This was also recently demonstrated for 3HAMP-CatIBs of *Pf*BAL, which were shown to be more suitable for the synthesis of (*R*)-benzoins in a biphasic system, than the corresponding TDoT-*Pf*BAL CatIBs, even outperforming the soluble, purified enzyme.[11a]

Single CatIBs of *Pf*BAL and *R*ADH outperform the corresponding Co-CatIBs in cascade reactions yielding PPD

Prompted by the above presented promising results, all of the generated (Co-)CatIBs were tested concerning their performance in the synthesis of PPD using the two-enzyme one-pot recycling cascade set up (Scheme 1, A). To directly compare cascade performance using single CatIBs of *Pf*BAL and *R*ADH, respectively, *Pf*BAL/*R*ADH Co-CatIBs, and the corresponding soluble enzyme controls, all enzyme variants were supplied in equivalent activity concentration, as determined for the *Pf*BAL/*R*ADH Co-CatIBs, with a fixed *Pf*BAL/*R*ADH ratio (see Table 1). The activity concentration (in µM; per subunit) per cascade reaction was determined by taking the protein content of the respective enzyme preparations (lyophilizates of soluble enzymes or (Co-)CatIBs)) into account as well as the residual activity of the (Co-)CatIBs relative to the activity of the soluble enzymes (set to 100%) (see Table S2). In an initial experimental set up, the single CatIBs

10.1002/adsc.201900189

(TDoT and 3HAMP) and the corresponding TDoT and 3HAMP Co-CatIBs were used under identical conditions at pH 8.0 as described recently for the use of the TDoT-derived *Pf*BAL/*R*ADH Co-CatIBs.[11b]

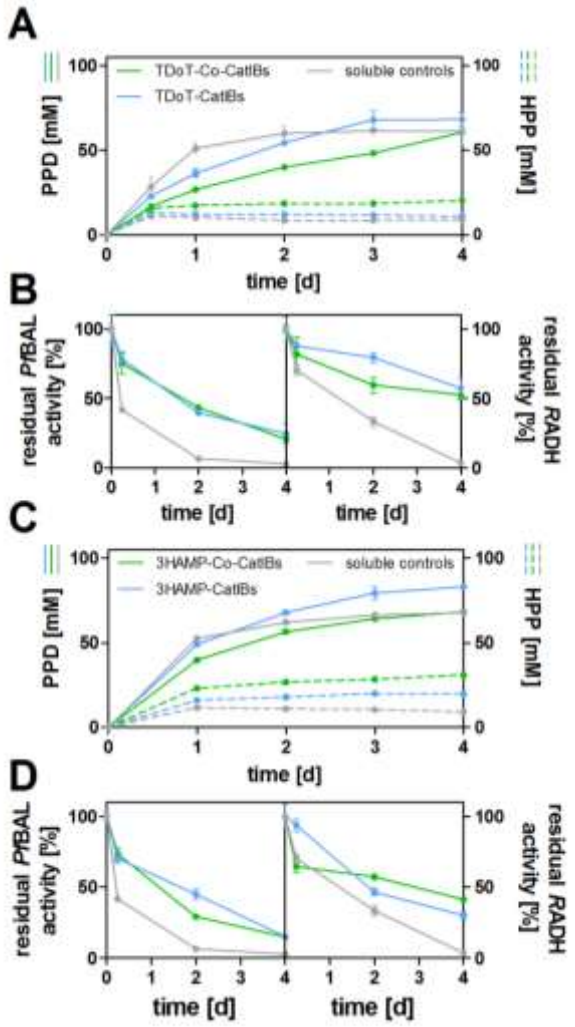

Figure 2. Two-enzyme one-pot recycling cascade for the production of PPD (solid lines in A and C) performed at pH 8.0 using TDoT-(Co-)CatIBs (A) and 3HAMP-(Co-)CatIBs (C). For reaction condition Experimental Section. In addition to the product PPD, also the intermediate HPP (dashed lines in A and C) was quantified. For quantification of benzaldehyde and benzoin see ESI Figure S1. Stability of *Pf*BAL (left) and *R*ADH (right) in (B) TDoT-(Co-)CatIBs and (D) 3HAMP-(Co-)CatIBs. The residual activies under reaction conditions and the activity at a given time point were measured with orthogonal assays and expressed relative to the activity of the respective enzyme preparation before starting the cascade reaction (see Experimental Section). All panels also contain data for the corresponding soluble control set-up (grey, solid and dashed lines), using *Pf*BAL and *R*ADH in an equivalent activity concentration. For comparison, the previously obtained results with TDoT Co-CatIBs are included in panel A (green solid and dashed line; see also Figure 4, g in [11b]). The employed catalyst concentrations are given in Table 1 and Table S2, entries 1-6. Error bars correspond to the standard deviation of the mean of three independent reactions. For details see the Experimental Section.

Under these conditions, we previously observed suboptimal conversion and the accumulation of the intermediate HPP, derived from the carboligation of benzaldehyde and acetaldehyde by *Pf*BAL (Scheme 1, A). Figure 2 displays the results obtained with all (Co-)CatIBs and the conversion curves following the intermediate HPP and the chiral target product PPD (diastereomeric excess (*de*) for 1*R*,2*R*-PPD in all cases >99%; data not shown). The overall conversion based on the total amount of benzaldehyde (10 mM) and benzyl alcohol (120 mM) is summarized in Table 1. In all cases, the use of single CatIBs (Figure 2, A and C; solid blue lines), even though supplied in equivalent activity concentrations as in the corresponding Co-CatIBs, resulted in higher overall conversions compared to all tested Co-CatIBs (Figure 2, A and C; solid green lines). After 4 days of reaction time about 68 mM and 83 mM PPD, respectively, were produced by the single TDoT- and 3HAMP-CatIBs, which corresponds to overall conversions of about 52% and 64%, respectively (Table 1, entries 1 and 4). During the same reaction time, only about 61 mM and 68 mM PPD, corresponding to overall conversions of 47% and 52%, respectively, were obtained by using TDoT and 3HAMP Co-CatIBs. Moreover, in all cases the 3HAMP (Co-)CatIBs outperformed the TDoT (Co-)CatIBs with regard to overall PPD yield (Figure 2, Table 1, entries 2 and 5). The control reactions, containing equivalent amounts of purified, soluble *Pf*BAL and *R*ADH gave similar conversions to PPD like the Co-CatIBs, corresponding to only 81-90% of the conversion yields obtained with the single CatIBs (Table 1, entries 1-6). As demonstrated in Figure 2 the reaction with the soluble enzymes initially proceeded faster until a plateau was reached after 2 days, after which no significant further formation of PPD was observed (Figure 2 B,C). The somewhat slower conversion observed for both CatIBs and Co-CatIBs might be related to diffusional/mass transfer limitation which is known for enzyme immobilizates in general [12] and for CatIBs in particular.[11f] In all cases tested with this intial setup significant amounts of the cascade intermediate HPP accumulated during the course of the reaction (Figure 2, A and C; dashed lines; Table 1, entries 1-6). A further by-product was benzoin, formed by *Pf*BAL catalysis from two molecules of benzaldehyde.[7c, 13] Benzoin accumulated to 0.015 mM in cascades employing 3HAMP-Co-CatIBs, but was not observed with the other enzyme preparations (ESI, Figure S1). The formation of side products is an undesired effect as the atom efficiency of the cascade is decreased and the workup of the final product is complicated. In the present case the formation of benzoin suggests that both enzymes are most probably inactivated under the reaction conditions, since the theoretically possible conversion could not be achieved. Benzoin is a known intermediate of the *Pf*BAL reaction during the formation of HPP and usually disappears during the course of the reaction with excess acetaldehyde.[14] This was also observed here directly under cascade

reaction conditions where soluble *Pf*BAL and *R*ADH were completely inactivated after 2 or 4 days, respectively (Figure 2, B, D; grey line). In contrast, under the same conditions all (Co-)CatIBs showed increased stability (Figure 2, B, D; green and blue lines). The accumulation of the intermediate HPP, moreover, suggests that the *R*ADH-catalyzed part of the cascade is specifically limiting under the employed reaction conditions. This can be improved by altering the *Pf*BAL/*R*ADH ratio. This, however, is not feasible for Co-CatIBs, as the *Pf*BAL/*R*ADH ratio is determined by the relative expression yields and fixed by the co-expression strategy.[11b] Therefore, in the following experiments, only single *Pf*BAL and *R*ADH CatIBs were employed, where the *R*ADH/*Pf*BAL ratio was increased by keeping the *R*ADH concentration constant, while reducing the amount of *Pf*BAL (Table 1, entries 7-12).

pH optimization of the cascade

For the here presented two-enzyme one-pot recycling cascade, in particular the pH value is critical, since for both enzymes the pH-optima of initial rate activities differ from the stability optima. The pH-optimum of *Pf*BAL has been investigated for both benzoin cleavage (lyase reaction) in the presence of acetaldehyde resulting in the formation of HPP as well as benzoin formation (ligase reaction) from benzaldehyde.[13] In both cases, *Pf*BAL showed an activity optimum at pH 8.0, with rapidly decreasing activities at more acidic pH values. At pH 9.0 the enzyme still retains about 80% of the maximum activity.[13] Regarding stability, soluble *Pf*BAL was shown to be stable between pH 6.0 and pH 8.0, but rather instable at pH 9.0 (10% residual activity after 27 h).[13] Soluble *R*ADH exhibits different pH-optima for reductive and oxidative reactions.[8] Kulig *et al.* found a broad pH optimum between pH 6 and 9.5 for the reduction of benzaldehyde, whereas a sharp pH optimum around pH 10.5 was found for the oxidation of cyclohexanol.[8] At pH 9.0 the enzyme showed a half-life of 20 h whereas at pH 9.5 *R*ADH was rapidly inactivated.[8] The low stability of the soluble enzyme at alkaline pH collides with the necessity of *R*ADH to catalyze both the reduction of HPP and the oxidation of benzyl alcohol efficiently in the 2-step cascade (Scheme 1, A), which requires a pH around 9 to enable both *R*ADH-catalyzed reactions (part I of the paper).[6] It must be mentioned that the reported stabilities were measured just in buffer and the presence of aldehydes most probably will further decrease the enzyme stability.

Therefore, to optimize cascade performance and to elucidate the pH-dependent stability of *Pf*BAL and *R*ADH under reaction conditions, the cascade was performed at different pH values (7.5 and 9.0), while, as before, the stabilities of all enzyme preparations were analyzed concomitantly. At pH 7.5 and pH 8.0 (see above) *Pf*BAL and *R*ADH in single CatIBs and Co-CatIBs clearly showed increased stability compared to the soluble enzymes, in most cases retaining up to or more than 50% residual activity after two days of reaction time (Figure 2 and ESI, Figure S2, B and D; ESI Table S3). At pH 9 the differences in stability converge, specifically for the *Pf*BAL variants, whereas both single *R*ADH CatIBs show similar but higher stability than the soluble enzyme (ESI, Figure S2, B and D).

At all tested pH-values, the *Pf*BAL preparations were less stable compared to *R*ADH under the tested conditions. The rapid inactivation of *Pf*BAL can be explained by the inactivation of the free enzyme by the employed aldehyde substrates.[7d] This explains the decelerated conversion after 2 days, which was only observed for the cascades performed with the soluble enzymes (Figure 2, Figure 4, ESI Figure S2, B and D, respectively).

The reaction rates and total conversions of the cascade increased from pH 7.5 to pH 9.0 (Figure 2 and ESI, Figure S2, B and D, Table 1) and thus show the inverse pattern observed for the stability of both enzymes. Maximal conversion (76%) was achieved at pH 9.0 using TDoT-CatIBs (ESI, Figure S2, C; Table 1, entry 10). Concomittantly, the accumulation of HPP was reduced to 2-3.6 mM after 4 days of reaction time (ESI, Figure S2, C; dashed lines), which is significantly lower than observed at pH 7.5 and pH 8.0 (Figure 2, ESI, Figure S2, Table 1). Again the formation of benzoin was neglegtable and only observed with the 3HAMP-(Co-)CatIBs at pH 9.0 (ESI, Figure S3). Although *Pf*BAL and *R*ADH show the lowest stability at pH 9.0, the better performance of the cascade at this pH is most probably due to the higher activity of *R*ADH specifically with respect to the oxidation of benzyl alcohol. Unfortunately, CatIB formation did not significantly increase the stability of the enzymes at pH 9.0, whereas pronounced stabilization was observed at pH 7.5 and pH 8.0 (Figure 2, B and D, ESI, Figure S2, B).

Addition of 2.5 vol% DMSO improved *R*ADH stability and cascade performance

It is known that for many enzymes, the addition of organic co-solvents can influence activity and stability.[15] As shown earlier, 20-30 vol% dimethyl sulfoxide (DMSO) in the aqueous buffer showed significant stabilizing and activity enhancing effects on soluble *Pf*BAL.[7c, 13]

However, under these conditions *R*ADH is not active and already 5 vol% DMSO diminished the activity to about 43% of the activity observed in buffer.[4c] To further optimize the *R*ADH part of the two-enzyme cascade, we therefore tested the influence of small amounts (2.5 vol%) of DMSO and methyl *tert*-butyl ether (MTBE) and comparatively

10.1002/adsc.201900189

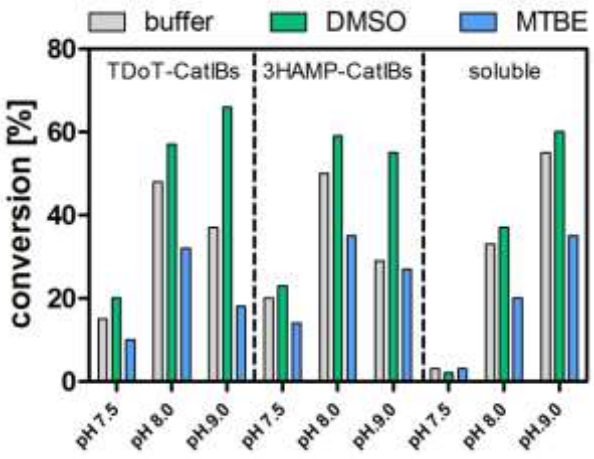

Figure 3. Evaluation of the *R*ADH-catalyzed reduction of HPP to PPD in 50 mM TEA buffer (grey bars), in the presence of 2.5 vol% DMSO (green bars) and 2.5 vol% MTBE (blue bars). Reactions were performed at pH 7.5, pH 8.0, and pH 9.0 as indicated. Details can be found in Experimental Section.

analyzed the formation of PPD from HPP catalyzed by *R*ADH (Figure 3, for half-lives under cascade reaction conditions see SI Table S3). All tests were performed at pH 7.5, 8.0, and 9.0. Interestingly, for soluble *R*ADH, addition of DMSO had no significant effect on the *R*ADH-catalyzed conversion of HPP, while addition of MTBE even resulted in about 40% lower conversions relative to TEA-buffer without organic co-solvent. The effects observed for the *R*ADH-CatIBs were more variable. For both the TDoT- and the 3HAMP-derived *R*ADH-CatIBs, addition of MTBE yielded lower conversion at all tested pH values compared to the buffer control. Also, addition of DMSO resulted only in a marginal increase in conversion at pH 7.5 and 8.0. However, at pH 9.0, where the cascade in buffer yielded already the best results but *R*ADH also showed the lowest stability, addition of DMSO was surprisingly beneficial, resulting in about 2-fold higher conversion compared to the reaction in TEA-buffer.

In conclusion, for the *R*ADH-part of the cascade, and most importantly for the *R*ADH CatIBs, addition of 2.5 vol% DMSO at pH 9.0 appears to be beneficial. Therefore, a final experiment was performed in which all CatIBs and Co-CatIBs were compared under these optimized reaction conditions (Figure 4). All reactions were performed at pH 9.0 in the presence of 2.5 vol% DMSO, and the reaction time was increased to 8 days to allow for maximal conversion of the substrates. Single CatIBs of *Pf*BAL and *R*ADH were supplied in amounts similar to the experiment performed in the absence of DMSO (ESI, Figure S2, C; see also Table 1, Table S2). Co-CatIBs were supplied at a fixed activity concentration of *R*ADH of 3 µM, which unavoidably results in an increased *Pf*BAL supply as compared to the single CatIBs, where the relative amount of *Pf*BAL is adjustable (Table 1, entries 15 and 16). Under these optimized reaction conditions the TDoT-derived single CatIBs gave the best conversion of 90.5-93% (after 4-8 days; Figure 4, A; Table 1 entry 13), resulting in a PPD yield of 121 mM after 8 days.

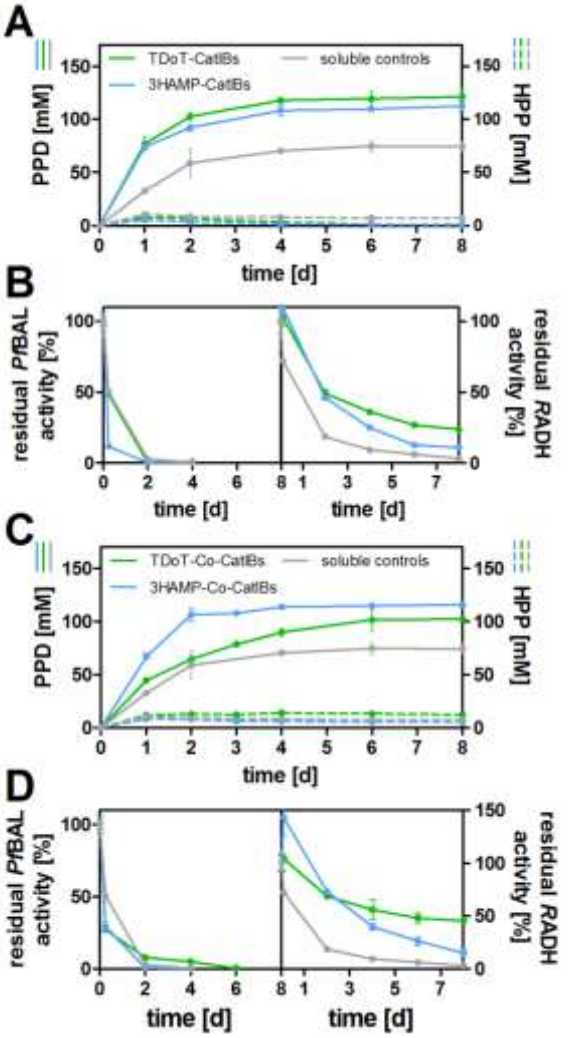

Figure 4. Optimized two-enzyme one-pot recycling cascade reaction for the production of PPD (solid lines in A and C) performed at **pH 9.0** in the presence of 2.5 vol% DMSO using (**A**) TDoT- and 3HAMP-CatIBs as well as the corresponding (**C**) Co-CatIBs. For further reaction condition see Experimental Section. In addition to the PPD product, also the cascade intermediate HPP (dashed lines in A and C) was quantified. For quantification of benzaldehyde and benzoin see ESI Figure S4. Stability of *Pf*BAL (left) and *R*ADH (right) in TDoT-(Co-)CatIBs (**B**) and 3HAMP-(Co-)CatIBs (**D**). All panels also contain data for the corresponding soluble control set-up (grey, solid, and dashed lines), using equivalent activity concentrations of *Pf*BAL and *R*ADH. The employed catalyst concentrations are given in Table 1 and Table S2 entries 13-17. Error bars correspond to the standard deviation of the mean of three independent reactions.

Table 1. Comparison of all cascade reactions performed in this study. PPD formation, overall conversion (in %) as determined relative to the sum of the employed aromatic substrates (benzaldehyde: 10 mM, benzyl alcohol: 120 mM) and HPP formation using TDoT- and 3HAMP (Co-)CatIBs, single CatIBs and the corresponding soluble enzymes determined after 4 d (8 d). Reactions were performed as described in the Experimental Section. Errors correspond to the standard deviation of the mean derived from 3 independent cascade reactions. [a:] activity concentration determined by taking the protein content and the active fraction of the corresponding enzyme/(Co-)CatIB lyophilisate into account (see Table S2).

entry	reaction conditions	*Pf*BAL [µM][a]	*R*ADH [µM][a]	*R*ADH/ *Pf*BAL	PPD [mM]	PPD conv. [%]	HPP [mM]
	pH 8.0						
1	TDoT-CatIBs	1.5	3.0	2	68.3±4.1	52.4±3.2	10.9±0.4
2	TDoT-Co-CatIBs	1.6	3.0	2	60.8±1.4	46.8±1.1	20.4±0.3
3	soluble control	1.4	3.0	2	61.3±7.8	47.1±6.0	8.9±0.1
4	3HAMP-CatIBs	0.8	3.0	4	83.1±0.4	63.9±0.3	19.8±0.1
5	3HAMP-Co-CatIBs	0.8	3.0	4	68.2±0.9	52.2±0.7	31.0±1.9
6	soluble enzyme control	0.7	3.0	4	67.7	52.1	9.2
	pH 7.5						
7	TDoT-CatIBs	0.6	3.0	5	64.5±0.9	37.9±3.5	10.0±0.1
8	3HAMP- CatIBs	0.6	3.0	5	49.3±4.5	49.6±0.7	14.0±0.3
9	soluble enzyme control	0.5	3.0	6	52.7	40.6	9.5
	pH 9.0						
10	TDoT-CatIBs	0.6	3.0	5	99.0±1.3	76.2±1.0	1.9±0.3
11	3HAMP-CatIBs	0.6	3.0	5	90.7±1.5	69.8±1.2	2.1±0.2
12	soluble enzyme control	0.5	3.0	6	92.6±1.5	71.2±1.2	3.6±0.2
	pH 9.0 / 2.5% (v/v) DMSO				**PPD**		**HPP**
					[mM]	**conv. [%]**	**[mM]**
					4 d (8 d)	**4 d (8 d)**	**4 d (8 d)**
13	TDoT-CatIBs	0.5	3.0	6	117.6±1.9 (121.2±8.2)	90.5±1.4 (93.2±6.3)	3.4±0.3 (0.6±0.1)
14	3HAMP- CatIBs	0.5	3.0	6	108.4±5.2 (112.4±4.7)	83.4±4.0 (86.5±3.6)	1.6±0.2 (1.3±0.5)
15	TDoT-Co-CatIBs	1.6	3.0	6	89.7±4.0 (102.2±2.5)	69.0±3.1 (78.7±1.9)	13.7±0.5 (12.0±1.2)
16	3HAMP-Co-CatIBs	0.9	3.0	2	113.5±2.6 (115.9±1.3)	87.3±2.0 (89.1±1.0)	5.9±0.3 (5.1±0.2)
17	soluble enzyme control	0.5	3.0	3	70.2±2.0 (74.4 ± 4.6)	54.0±1.5 (57.2±3.5)	8.0±0.8 (7.1±1.0)

Similar results were obtained for the 3HAMP-derived (Co-)CatIBs, albeit with slightly lower overall PPD yields (112-115 mM PPD, 86.5-89% conversion) (Figure 4, A, Table 1 entries 14 and 16). Application of the 3HAMP Co-CatIBs yielded higher conversions as the corresponding TDoT-derived Co-CatIBs (Figure 4, C, Table 1 entry 15 and 16). However, compared to the cascade reaction performed with single CatIBs (Table 1, entries 13, 14) clearly increased amounts of HPP accumulated during the reactions catalyzed by the Co-CatIBs (Table 1, entries 15 and 16). This can be explained by the higher activity of *Pf*BAL relative to *R*ADH within those Co-CatIBs. Hereby, it is obvious that the highest HPP concentration (13.7 mM) was formed with TDoT-Co-CatIBs, containing the highest *Pf*BAL activity concentration in the tested series (Table 1, entry 15).Under these optimized conditions all CatIBs clearly outperformed the soluble enzymes, which, when applied in equivalent activity concentration, yielded only about 70 mM PPD (57% conversion) within 8 days, thereby accumulating approx. 7 mM HPP (Table 1, entry 17). The increased conversions, which were observed for all (Co-)CatIB preparations hereby appear to be related to an increase in stability specifically of the *R*ADH in (Co-)CatIBs in the presence of 2.5 vol% DMSO (Figure 4, B and D; compared to ESI, Figure S2, B and D for the reactions without DMSO; for half-lives see Table S3). Using the best setup (TDoT single CatIBs, pH 9.0, 2.5 vol% DMSO); PPD was prepared and isolated at a larger scale (see ESI, Supporting Methods). Product identity and purity was verified by ^{1}H- and ^{13}C-NMR and chiral GC (ESI, Figure S7/S8).

Conclusion

In the present contribution, a two-enzyme one-pot recycling cascade for the production of the vicinal 1,2-diol (1*R*,2*R*)-1-phenylpropane-1,2-diol (PPD) was optimized. As for most one-pot cascade reactions a facile balance between enzyme activity and enzyme stability proved instrumental for optimal cascade performance, where, in the present case, optimal conversion was limited by deviating pH optima and stabilities of the two employed enzymes. The problem was here mainly caused by the application of *R*ADH to catalyze the main reaction (reduction of HPP to PPD) and also cofactor regeneration through

oxidation of benzylalcohol. As a consequence of the diverging pH optima for reduction and oxidation, pH 9 represents a compromise to enable both reactions with sufficient activity. However, concomitantly this results in reduced stability of both enzymes. Stabilization of *Pf*BAL can be achieved by addition of organic cosolvents, as was deduced from previous studies.[7c, 13] Soluble *Pf*BAL hereby requires 20-30 vol% of DMSO for stabilization, which, however, is by far too much for *R*ADH to remain active.[4c]

The inherent stability problem was therefore here addressed by employing catalytically active inclusion bodies (CatIBs) of *Pf*BAL and *R*ADH, which, compared to the soluble, purified enzymes, show improved stability.[11b] After optimization of the reaction pH, the *R*ADH/*Pf*BAL ratio and the co-solvent content, we could demonstrate that almost full conversion (>90%), corresponding to the theoretically possible conversion calculated in part I of this paper,[6] was possible with both TDoT- and 3HAMP-CatIBs operating in the presence of low DMSO concentrations (2.5 vol%) at 30 °C. Specifically the stability of *R*ADH-CatIBs benefits from the added DMSO at pH 9 (Figure 3 and 4). Besides *Pf*BAL-CatIBs were not stabilized under these condition. However, it can be assumed that due to the high activity of this enzyme,[16] even immobilized in CatIBs, the conversion is still faster than the inactivation rate. At the end of the reaction with TDoT-CatIBs the *R*ADH CatIBs still showed 50% residual activity and could principally be reused (see SI, Table S2). The instability of *Pf*BAL under optimized conditions now limits the cascade with regard to improved space-time yields and at present prohibits the recycling of the catalyst in batch. Further experiments would be needed to optimize the stability of the *Pf*BAL-CatIBs, which could be achieved e.g. by cross-linking [17] or magnetization.[18]

Experimental Section

Materials

Chemicals and enzymes were purchased from Sigma-Aldrich, Fluka, Roth, Biosolve, Alfa Aesar, AppliChem, Merck, and Thermo Scientific (Waltham, MA, USA). Enantiopure (*R*)-(3,3‘,5,5‘)-tetramethoxy benzoin (TMBZ) was taken from a stock prepared as described elsewhere.[11a] Enantiopure (*R*)-2-hydroxy-1-phenylpropane-1-one (HPP) and (1*R*,2*R*)-1-phenylpropane-1,2-diol (PPD) was synthesized as described before (HPP [4b]; PPD [19]).

Construction of expression plasmids and production of (Co-)CatIBs and soluble control proteins

The construction of the different (co-)expression plasmids,[11a-c, 11f] the production of (Co-)CatIBs as well as of the corresponding soluble control proteins in *E. coli* and their subsequent purification[11a, 11b, 11f] was described before. Details can be found in the ESI, Supporting Methods section.

Cell fractionation and determination of (Co-)CatIB formation efficiency

The efficiency of (Co)-CatIB formation was evaluated by quantifying *R*ADH- or *Pf*BAL-activity in the different *E. coli* cell extract fractions after cell disruption as described before.[11b] In brief, the crude cell extract (CE), obtained by cell lysis, was separated in the soluble-protein containing supernatant fraction (S) and the insoluble, IB-containing pellet fraction by centrifugation (2 min, 7,697 *xg*, room temperature) employing suitable CE dilutions in lysis buffer (50 mM Na_2PO_4, 100 mM NaCl, pH 8.0). The resulting pellet was washed once with lysis buffer, centrifuged (2 min, 7,697 *xg*, room temperature) and resuspended in the initial volume of lysis buffer, resulting in the final insoluble IB-containing pellet fraction (I), for which activities were measured. The activities in the S and I fractions were expressed relative to the activity of the CE fraction (set to 100%). *R*ADH and *Pf*BAL activity was determined in 4x10 mm quartz-glass fluorescence cuvettes using a continuous fluorometric activity assay by employing a Fluorolog3-22 spectrofluorometer (Horiba Jobin Yvon, Bensheim, Germany) at front-face angle geometry as described before.[7d, 11b] *R*ADH activity was measured by following the reduction of cyclohexanone to cyclohexanol (ESI, Scheme S1, A) by monitoring the consumption of the cofactor NADPH recorded for 90 s at 30 °C by excitation at λ_{ex} = 350 nm and emission at λ_{em} = 460 nm (bandwidth 1.4 nm in excitation and emission). Reactions contained 100 mM cyclohexanone, 0.2 mM NADPH, and 200 µl sample in TEA-buffer (50 mM TEA, 0.8 mM $CaCl_2$, pH 7.5) in a volume of 1 ml. For measuring the *Pf*BAL activity the carboligation of 3,5-dimethoxybenzaldehyde (DMBA) to (*R*)-1,2-bis(3,5-dimethoxyphenyl)-2-hydroxyethanone (TMBZ) (ESI, Scheme S1, B) was monitored for 90 s at 25 °C by excitation at λ_{ex} = 350 nm and emission at λ_{em} = 460 nm (bandwidth 1.3 nm in excitation and emission) with 3 mM DMBA (in DMSO, final concentration 20% (v/v)) and 200 µl sample in TEA-buffer (50 mM TEA, 0.5 mM ThDP, 2.5 mM $MgSO_4$, pH 8.0) in a volume of 1 ml. All measurements were performed at least as four technical replicates of biological triplicates.

Determination of specific enzyme activities and stability investigations

*R*ADH and *Pf*BAL-activity assays were used to determine the residual activity of the different (Co-)CatIB preparations relative to the respective soluble, purified enzyme. Likewise, those assays were employed for stability investigations, performed during the cascade reactions, to determine the stability of the respective enzyme preparation under varying reaction conditions. The employed assays have been described before.[11b]

In brief, initial *R*ADH rate activities were measured by a discontinuous photometric assay following the reduction of cyclohexanone to cyclohexanol, whereby the consumption of the NADPH-cofactor was measured photometrically at

340 nm (ESI, Scheme S1, A). The molecular extinction coefficient of NADPH was determined under assay conditions ($\varepsilon_{340\,nm}$ = 1975 mM^{-1} cm^{-1}). The assay buffer (volume 1400 µl) contained 0.4 mM NADPH and 100 mM cyclohexanol, in 1750 µl TEA-buffer (50 mM, 0.8 mM $CaCl_2$, pH 7.5), pre-tempered to 30 °C. Reactions were started by addition of 350 µl pre-tempered enzyme sample ((Co-)CatIBs, or soluble *R*ADH) in suitable dilutions. Reactions were incubated for 5 min at 30 °C and 1000 rpm (Thermomixer comfort, Eppendorf, Germany), under sampling (250 µl) every minute. To stop the reaction, samples were diluted 1:3 with 500 µl methanol, centrifuged (5 min, 7697 *xg*, room temperature), and the NADPH-specific absorption was measured in standard disposable half-micro cuvettes. Initial *Pf*BAL rate activities were determined by following the carboligation of 3,5-dimethoxy benzaldehyde (DMBA) to (*R*)-(3,3‘,5,5‘)-tetramethoxy benzoin (TMBZ) (ESI, Scheme S1, B) by using a discontinuous HPLC assay.[7d] The assay solutions (volume 800 µl), contained 80% (v/v) TEA-buffer (50 mM, 2.5 mM $MgSO_4$, 0.1 mM ThDP, pH 7.5), 20% (v/v) DMSO, and 10 mM DMBA, pre-tempered at 30 °C. The reactions were started by adding 200 µl pre-tempered enzyme sample ((Co-)CatIBs, or soluble *Pf*BAL) in suitable dilutions. Reactions were incubated for 5 min at 30 °C and 1000 rpm (Thermomixer comfort, Eppendorf, Germany) under sampling (20 µl) every minute. Reactions were stopped by 1:10 dilution with methanol (including 0.1‰ (v/v) *p*-methoxy benzaldehyde (*p*-MBA) as internal standard) and analysed by high performance liquid chromatography (HPLC, see Experimental Section: *HPLC analysis*). For calibration data see ESI Figure S5.

The stability of different enzyme preparations ((Co-)CatIBs, or soluble enzyme) during the cascade reaction was determined using those assays and calculated as residual activity relative to the starting activity, as described previously.[11b] In brief, (Co-)CatIBs were removed from the cascade reaction medium by centrifugation (2 min, 7697 *xg*, room temperature) and resuspended in the fresh assay buffer in suitable concentrations. Samples of the soluble control were directly diluted in the respective buffers. For quantification of the stability, activities are given relative to the starting activity of the enzymes (before addition of the cascade reactions substrates). All reactions were performed in triplicate using three separate samples of the same preparation.

RADH-catalyzed reactions in presence of DMSO and MTBE

To evaluate the influence of organic co-solvents such as dimethyl sulfoxide (DMSO) and methyl *tert*-butyl ether (MTBE) on the efficacy of the *R*ADH-catalyzed reaction step (HPP to PPD) as well as on the cofactor regeneration reaction, we directly determined PPD formation from HPP (Scheme 1, A). All experiments were carried out under conditions similar to the corresponding cascade reactions at pH 7.5, 8.0, and 9.0. The reactions (volume 1 ml) were carried out in the respective assay buffer (see Experimental Section: *Cascade reaction optimization*), supplemented with 10 mM HPP, 120 mM benzyl alcohol, and 0.2 mM $NADP^+$. The influence of organic cosolvents was tested by addition of 2.5 vol% DMSO and MTBE, respectively. In order to quantitatively compare the conversion by the soluble purified *R*ADH to the conversion catalyzed by the corresponding CatIBs, 0.05 U ml^{-1} *R*ADH was used. This corresponds to: 0.73 mg ml^{-1} TDoT-*R*ADH, 0.26 mg ml^{-1} 3HAMP-*R*ADH, and 0.03 mg ml^{-1} soluble *R*ADH. Reactions were carried out as described for the cascade reactions (see Experimental Section: *Cascade reaction optimization*) at 30°C and 1000 rpm for 1 d. Samples were prepared and analysed by HPLC as described below.

Cascade reaction optimization

General reaction setup

The general reaction setup for the synthesis of PPD from benzaldehyde and acetaldehyde using co-immobilized CatIBs (Co-CatIBs) of *Pf*BAL and *R*ADH has been described before.[11b] In brief, all reactions have been performed in 50 mM TEA buffer at different pH values (pH 7.5, pH 8.0, or pH 9.0) supplemented with 0.5 mM ThDP, 2.5 mM $MgSO_4$, and 0.8 mM $CaCl_2$. Acetaldehyde (150 mM) and benzaldehyde (10 mM) were added as substrates as well as benzyl alcohol (120 mM) as a cosubstrate. Oxidation of benzyl alcohol delivers redox equivalents for the substrate-coupled cofactor regeneration catalyzed by *R*ADH, thereby generating benzaldehyde as a substrate for the *Pf*BAL-catalyzed first reaction step. All reactions were set up in sealed glass vials, to avoid evaporation of aldehyde substrates, containing a total volume of 1 ml. Reactions were incubated at 30 °C and 1000 rpm over a period of up to 8 days (Thermomixer comfort, Eppendorf, Germany). All reactions contained 0.5 U ml^{-1} *R*ADH, corresponding to an *R*ADH activity concentration of 3 µM, but variable amounts of *Pf*BAL (see Table 1/Table S2) (activity measured with the orthogonal assays, see Experimental Section: *Determination of specific enzyme activities and stability investigations*). Reactions were started by addition of the enzymes.

To follow the reaction progress, 20 µl samples, drawn at specific time points from freshly opened and afterwards discarded aliquots, were mixed with 180 µl methanol (including 0.1‰ (v/v) *p*-methoxy benzaldehyde (*p*-MBA) as internal standard). Samples were then vortexed and centrifuged to remove residual aggregates, and analysed by high performance liquid chromatography (HPLC). To analyse the stability of the corresponding enzyme preparations ((Co-)CatIBs or soluble *Pf*BAL/RADH) under cascade reaction conditions, the residual activity of the employed enzyme preparation (relative to the starting activity) was determined at specific time points using orthogonal assays. All cascade reactions using (Co-)CatIBs were performed in triplicate using three separate CatIB samples of the same preparation.

To optimize conversion and reduce formation of the HPP intermediate, the, cascade operating conditions were optimized with regard to the employed (Co)-CatIB construct, $NADP^+$ concentration, volumetric activity of the employed enzyme preparations, reaction pH and addition of co-solvents:

a) Initial experiments at pH 8
Initially, to compare different *Pf*BAL/*R*ADH (Co)-CatIB preparations, cascade reactions were performed in an identical manner as described by Jäger *et al.*,[11b] using 50 mM TEA buffer pH 8.0 supplemented with ThDP, $MgSO_4$ and $CaCl_2$ as described above. $NADP^+$ was provided at a concentration of 0.3 mM. In all cases *R*ADH was employed at a fixed volumetric activity of 0.5 U ml^{-1}, corresponding to 3 µM active *R*ADH (Table1/Table S2).
To directly compare cascade performance between reactions carried out using single CatIBs, Co-CatIBs, and the corresponding soluble controls, soluble *Pf*BAL, and single *Pf*BAL-CatIBs were supplied in amounts to yield the same volumetric activity (and therefore the same activity concentration) as the Co-CatIBs, where the *Pf*BAL/*R*ADH ratio cannot be adjusted. The employed catalyst concentrations are listed in Table 1/Table S2.

b) pH optimization
To evaluate the influence of the buffer pH on the cascade performance and enzyme stability, the reactions were additionally carried out at pH 7.5 and pH 9.0. For the reactions at pH 7.5 TRIS buffer (50 mM) was used, while the reactions at pH 9.0 were carried out in TEA buffer (50 mM). Both buffers were supplemented with ThDP, $MgSO_4$ and $CaCl_2$ as described above. $NADP^+$ was supplied at a concentration of 0.8 mM. In both cases 0.5 U ml^{-1} *R*ADH (3 µM active enzyme) and 2.8 U ml^{-1} *Pf*BAL (~0.6 µM active enzyme) were employed (Table 1/Table S2).

c) Optimized reaction cascade at pH 9.0 with DMSO as a co-solvent
A final set of experiments was carried out to compare the CatIBs and Co-CatIBs cascade performance under optimized conditions. Reactions were carried out in 50 mM TEA buffer supplemented with ThDP, $MgSO_4$ and $CaCl_2$ as described above. $NADP^+$ was provided at a final concentration of 0.8 mM as described above. Reactions were carried out in the presence of 2.5 vol% DMSO. As before a fixed *R*ADH volumetric activity of 0.5 U ml^{-1} (3 µM active enzyme) was used (Table 1/Table S2), while different volumetric *Pf*BAL activities were employed (2.5 U ml^{-1} for single TDoT- and 3HAMP-CatIBs (0.5 µM active enzyme); and variable U ml^{-1} for the corresponding Co-CatIBs; see Table 1/Table S2).

HPLC analysis
All HPLC samples were analyzed using a Thermo Scientific Dionex Ultimate 3000 HPLC system, equipped with a Diode Array detector DAD-3000 (both: ThermoFisher Scientific, Waltham, MA, USA) and Chiralpak® IE column (4,6 µm x 250 mm, 5 µm particle; pre-column: Chiralpak® IE; 4 mm x 10 mm; both Daicel, Tokyo, Japan). A binary mobile phase (A: dd H_2O and B: acetonitrile; flow rate 1 ml min^{-1}) was used for separation, employing two different protocols as described before.[11b]
For samples originating from cascade reactions, the following gradient was used: 15 vol% B for 8 min, 35 vol% B for 3 min, 60 vol% B for 3 min, and 15 vol% B for 3 min. Retention times: PPD: 210 nm, R_t = 11.2 min; HPP: 245 nm, R_t = 15.4 min; benzaldehyde: 245 nm, R_t = 16.2 min; benzyl alcohol: 210 nm, R_t = 10.2 min; benzoin: 210 nm, R_t = 18.5 min; *p*-MBA (internal standard): 270 nm, R_t = 17.1 min.
For HPLC samples originating from *Pf*BAL activity assays, DMBA and TMBZ were separated by isocratic elution (50 vol% B for 20 min). DMBA (R_t = 7.6 min) and TMBZ (R_t = 9.4 min) were detected at 215 nm, *p*-MBA (internal standard, R_t = 6.1 min) was detected at 270 nm. Quantification of all substrates and products were achieved by calibration using respective reference compounds (see ESI Figure S5).

Acknowledgements

We thank Stefanie Longerich (Heinrich-Heine-Universität Düsseldorf) for her help during the initial phases of the study, Ramona Kloß for the set-up of the HPLC analysis, and Prof. Wolfgang Kroutil (University of Graz, Austria) for providing the radh *gene. Furthermore, we thank Ursula Mackfeld (Forschungszentrum Jülich GmbH, IBG-1) for her excellent help with the work-up of PPD as well as GC and NMR analyses. This work was funded by the Bioeconomy Science Center (BioSC), which is financially supported by the Ministry of Culture and Science of North-Rhine Westphalia within the framework of the NRW Strategieprojekt BioSC (No. 313/32 3-400-002 13). BioSC is a research cluster consisting of the universities RWTH Aachen, Düsseldorf, and Bonn, and the Forschungszentrum Jülich.*

References

[1] M. Kurina-Sanz, F. R. Bisogno, I. Lavandera, A. A. Orden, V. Gotor, *Adv. Synth. Catal.* **2009**, *351*, 1842-1848.

[2] a) T. H. Johnson, K. C. Klein, *J. Org. Chem.* **1979**, *44*, 461-462; b) R. Noyori, I. Tomino, Y. Tanimoto, *J. Am. Chem. Soc.* **1979**, *101*, 3129-3131; c) Z. Wang, Y. T. Cui, Z. B. Xu, J. Qu, *J. Org. Chem.* **2008**, *73*, 2270-2274; d) M. Tokunaga, J. F. Larrow, F. Kakiuchi, E. N. Jacobsen, *Science* **1997**, *277*, 936-938; e) W. Notz, B. List, *J. Am. Chem. Soc.* **2000**, *122*, 7386-7387.

[3] a) D. Kihumbu, T. Stillger, W. Hummel, A. Liese, *Tetrahedron-Asymmetr* **2002**, *13*, 1069-1072; b) J. Kulig, R. C. Simon, C. A. Rose, S. M. Husain, M. Hackh, S. Ludeke, K. Zeitler, W. Kroutil, M. Pohl, D. Rother, *Catal. Sci. Technol.* **2012**, *2*, 1580-1589; c) S. M. Husain, T. Stillger, P. Dünkelmann, M. Lodige, L. Walter, E. Breitling, M. Pohl, M. Burchner, I. Krossing, M. Müller, D. Romano, F. Molinari, *Adv. Synth. Catal.* **2011**, *353*, 2359-2362.

[4] a) J. Wachtmeister, A. Jakoblinnert, D. Rother, *Org. Process Res. Dev.* **2016**, *20*, 1744-1753; b) A. Jakoblinnert, D. Rother, *Green Chem.* **2014**, *16*, 3472-3482; c) J. K. Kulig, Dissertation thesis, Heinrich-Heine Universität Düsseldorf **2013**.

[5] B. M. Choudary, N. S. Chowdari, S. Madhi, M. L. Kantam, *J. Org. Chem* **2003**, *68*, 1736-1746.

[6] J. Kulig, T. Sehl, U. Mackfeld, W. Wiechert, M. Pohl, D. Rother, *Adv. Synth. Catal.* **2019**, *361*, DOI: 10.1002/adsc.201900187.

[7] a) F. Hildebrand, S. Kuhl, M. Pohl, D. Vasic-Racki, M. Müller, C. Wandrey, S. Lutz, *Biotechnol. Bioeng.* **2007**, *96*, 835-843; b) T. Stillger, Dissertation thesis, University Bonn **2004**; c) P. Domínguez de María, T. Stillger, M. Pohl, S. Wallert, K. Drauz, H. Gröger, H. Trauthwein, A. Liese, *J. Mol. Catal. B-Enzym.* **2006**, *38*, 43-47; d) M. Schwarz, Dissertation thesis, Heinrich-Heine University Düsseldorf **2010**.

[8] J. Kulig, A. Frese, W. Kroutil, M. Pohl, D. Rother, *Biotechnol. Bioeng.* **2013**, *110*, 1838-1848.

[9] J. Stetefeld, M. Jenny, T. Schulthess, R. Landwehr, J. Engel, R. A. Kammerer, *Nat. Struct. Biol.* **2000**, *7*, 772-776.

[10] M. V. Airola, K. J. Watts, A. M. Bilwes, B. R. Crane, *Structure* **2010**, *18*, 436-448.

[11] a) R. Kloss, T. Karmainski, V. D. Jäger, D. Hahn, A. Grünberger, M. Baumgart, U. Krauss, K.-E. Jaeger, W. Wiechert, M. Pohl, *Catal. Sci. Technol.* **2018**, *8*, 5816-5826; b) V. D. Jäger, R. Lamm, R. Kloß, E. Kaganovitch, A. Grünberger, M. Pohl, J. Büchs, K.-E. Jaeger, U. Krauss, *ACS Synth. Biol.* **2018**, *7*, 2282-2295; c) V. D. Jäger, R. Kloss, A. Grünberger, S. Seide, D. Hahn, T. Karmainski, M. Piqueray, J. Embruch, S. Longerich, U. Mackfeld, K.-E. Jaeger, W. Wiechert, M. Pohl, U. Krauss, *Microb. Cell Fact.* **2019**, *18:33*; d) R. Kloss, M. H. Limberg, U. Mackfeld, D. Hahn, A. Grünberger, V. D. Jäger, U. Krauss, M. Oldiges, M. Pohl, in *Sci Rep*, *Vol. 8*, **2018**, p. 5856; e) U. Krauss, V. D. Jäger, M. Diener, M. Pohl, K.-E. Jaeger, *J. Biotechnol.* **2017**, *258*, 136-147; f) M. Diener, B. Kopka, M. Pohl, K. E. Jaeger, U. Krauss, *ChemCatChem* **2016**, *8*, 142-152.

[12] a) B. Schmieg, J. Döbber, F. Kirschhofer, M. Pohl, M. Franzreb, *Front. Bioeng. Biotechnol.* **2019**, *6*; b) R. A. Sheldon, J. M. Woodley, *Chem. Rev.* **2018**, *118*, 801-838.

[13] E. Janzen, M. Müller, D. Kolter-Jung, M. M. Kneen, M. J. McLeish, M. Pohl, *Bioorg. Chem.* **2006**, *34*, 345-361.

[14] A. S. Demir, M. Pohl, E. Janzen, M. Müller, *J. Chem. Soc. Perk. T. 1* **2001**, 633-635.

[15] M. T. Reetz, *J. Am. Chem. Soc.* **2013**, *135*, 12480-12496.

[16] T. Stillger, M. Pohl, C. Wandrey, A. Liese, *Org. Process Res. Dev.* **2006**, *10*, 1172-1177.

[17] J. Nahalka, A. Vikartovska, E. Hrabarova, *J. Biotechnol.* **2008**, *134*, 146-153.

[18] R. Koszagova, T. Krajcovic, K. Palencarova-Talafova, V. Patoprsty, A. Vikartovska, K. Pospiskova, I. Safarik, J. Nahalka, *Microb. Cell Fact.* **2018**, *17*.

[19] J. Kulig, R. C. Simon, C. A. Rose, S. M. Husain, M. Häckh, S. Lüdeke, K. Zeitler, W. Kroutil, M. Pohl, D. Rother, *Catal Sci Technol* **2012**, *2*, 1580-1589.

10.1002/adsc.201900189

FULL PAPER

An Enzymatic 2-Step Cofactor and Co-Product Recycling Cascade towards a Chiral 1,2-Diol. Part II: Catalytically Active Inclusion Bodies

Adv. Synth. Catal. **Year**, *Volume*, Page – Page

Vera D. Jäger[a,c], Maja Piqueray[a], Selina Seide[b,c], Martina Pohl[b,c], Wolfgang Wiechert[b,c], Karl-Erich Jaeger[a,b,c], Ulrich Krauss[a,c*]